A Drift-Diffusion Solver Using a Finite-Element Method to Analyze Carrier Dynamics at Ultra-high Solar Concentrations

Emily Carlson[1], Margaret Stevens[1], David Emerson[2], Xiaozhe Hu[2], James Adler[2], and Thomas E. Vandervelde[1*]
[1]Renewable Energy and Applied Photonics Laboratories, Electrical and Computer Engineering
[2]Math Department
Tufts University
Medford, Massachusetts, USA
*tvanderv@ece.tufts.edu

***Abstract*— We present a drift-diffusion and Poisson solver using a finite-element method to study carrier dynamics under ultra-high solar concentration. By modeling the carrier densities and the electric potential in quasi steady-state and dynamic conditions, we can use the splitting of the quasi-Fermi levels to model electrical properties such as open-circuit voltage. In this work, we analyze the validity of previously used approximations on open-circuit voltage and the effects of increasing optical carrier densities on small band gap solar cells. Graded mesh refinement is implemented to improve runtime. Ultimately, we show a change in the carrier profiles that may lead to detrimental charge carrier extraction.**

Keywords—photovoltaic cells; finite element analysis; numerical simulation; germanium.

I. INTRODUCTION

Concentrating photovoltaics (CPVs) are a low cost renewable energy option to compete with cheap fossil fuels. By generating comparable power in a decreased illumination area, they reduce cost without sacrificing power output. The present record for CPV efficiencies occurs in devices subject to solar concentrations greater than 500 suns [1]. At ultra-high solar concentrations, when solar concentration is greater than 1000 suns, we need to reexamine our understanding of the physics behind electrical properties of the cell. At these ultra-high concentrations, the devices move from the "low-injection" to "high-injection" regime as the number of optically generated carriers approach the equilibrium carrier densities. This changes our understanding of carrier dynamics and the dominant type of carrier transport in the device, as drift current begins to rival diffusion current [2].

Germanium (Ge) solar cells have been successfully used as the bottom junction for high-efficiency concentrator multijunction photovoltaics (MJPVs) [3]. With a small band gap of 0.661eV and intrinsic carrier concentration on the order of 10^{13} cm^{-3}, the performance of Ge solar cells is more sensitive to thermal [4] and Auger recombination [5] effects that limit device performance. Due to these complications, it is no longer trivial to model the open-circuit voltage V_{OC} in small band gap PV cells operating under ultra-high solar concentrations.

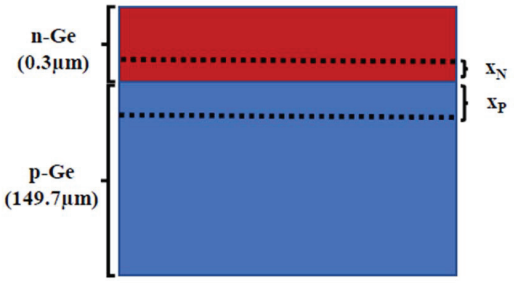

Fig. 1 Schematic of a simple germanium solar cell with the boundaries of the depletion region - x_N and x_P - shown. This image is not to scale.

For high irradiance (X > 100), it has been experimentally confirmed that the following approximation holds:

$$V_{oc} = \frac{nkT}{q}\ln\left(\frac{I_{sc}(X)}{I_0}+1\right) \approx V_{oc}^{\{1\ sun\}} + \frac{nkT}{q}\ln(X) \quad (1)$$

where n is the diode ideality factor, k is Boltzmann's constant, T is absolute temperature, q is the elementary charge, I_{SC} is short circuit current, I_0 is the diode reverse saturation current, and X is solar concentration [6].

However, for ultra-high solar concentrations the approximation in (1) should be reexamined. To test the validity of this expression for small band gap semiconductors at ultra-high irradiance, we use the definitions of quasi-Fermi levels (E_{Fn} and E_{Fp}) to model V_{OC} under quasi-steady state and dynamic conditions on a device of length L.

$$E_{F_n}(x,t) = E_i + kTln\left(\frac{n(x,t)}{n_i}\right) \quad (2)$$

$$E_{F_p}(x,t) = E_i - kTln\left(\frac{p(x,t)}{n_i}\right) \quad (3)$$

$$V_{oc}(t) = \frac{1}{q}\left(E_{F_n} - E_{F_p}\right) = \frac{kT}{q}\ln\left(\frac{n(0,t) - p(L,t)}{n_i^2}\right) \quad (4)$$

To better understand the effects of high-optical carrier generation on small band gap Ge solar cells, we built a drift-diffusion and Poisson solver to isolate the behavior of the optically generated carriers from any thermal processes. To investigate V_{OC} in small band gap semiconductor solar cells, we use a standard finite-element approach with Lagrange elements to create a flexible solver that iteratively computes n(x,t), p(x,t) and V(x,t) as a function of solar concentration. We extract V_{OC} from the computed quasi-Fermi levels and show its evolution with solar concentration can be modeled by (1). Additionally, we notice a change in device behavior when optically generated carriers begin to rival extrinsic carriers that could be exacerbating thermal degradation of electrical properties seen experimentally under ultra-high solar concentrations.

II. Problem Formulation

Our partial differential equation (PDE) system consists of two carrier continuity equations and Poisson's equation. The carrier concentrations of electrons (n) and holes (p) are

$$n(x,t) = n_0(x) + \delta n(x,t) \quad (5)$$

$$p(x,t) = p_0(x) + \delta p(x,t) \quad (6)$$

which can be interpreted as the superposition of the equilibrium concentrations and the optically generated carriers, δn and δp. The carrier continuity equations describe the flux of electrons and holes as a function of solar cell thickness and time. Poisson's equation characterizes the electric potential (V) that arises from carrier concentration profiles. Our PDE system is

$$\frac{\partial n}{\partial t} = \frac{1}{q}\frac{\partial}{\partial x}\left(qD_n\frac{\partial n}{\partial x} + q\mu_n n\frac{\partial V}{\partial x}\right) + G_{op} - U \quad (7)$$

$$\frac{\partial p}{\partial t} = \frac{1}{q}\frac{\partial}{\partial x}\left(qD_p\frac{\partial p}{\partial x} - q\mu_p p\frac{\partial V}{\partial x}\right) + G_{op} - U \quad (8)$$

$$\frac{\partial^2 V}{\partial x^2} = -\frac{q(p - n + N_D - N_A)}{\epsilon} \quad (9)$$

where D_n, D_p, μ_n, μ_p and ϵ are material parameters and N_D and N_A are the doping profiles of the n-type and p-type material, respectively. We will be using the material parameters of Ge for our model.

A. Computation Optimization

To handle the widely varying orders of magnitude in our problem, we implemented a nondimensionalization scheme based on the Debye length for space and the dielectric relaxation time constant for any time-stepping formulations [7]. Results for time-stepping formulations are shown in [8]. This introduces a scaling to the system, that increases robustness of the iterative process and improves the accuracy of the numerical solutions.

TABLE I. Runtime Comparisons

	Runtime (minutes:seconds)		
X	**Original code**	**GMR code**	**Improvement Factor**
10	26:03.85	2:07.44	11.65
10,000	26:45.00	2:11.58	12.20

Additionally, we implemented graded mesh refinement (GMR) since we know our system requires high refinement at both edges of our device. The area leading up to and including the depletion region ($0.3\mu m + x_p$) and a section of the same length at the end is more refined than the middle portion. For X=1 to X=10,000 the average runtime for the original code is 1568 seconds and the average runtime for GMR code is 130 seconds. This significantly decreased the runtime of our code and produces similar results, as seen in Table I and Fig. 2, respectively.

B. Generation and Recombination

Instead of the simplified uniformly illuminated condition, our generation profile varies spatially for optically generated carriers based on the Beer-Lambert Law [9]. Light intensity is attenuated as a function of depth through the material and the absorption coefficient, α, which is a material parameter. Therefore, our generated carrier profiles will also decay proportional to α, and our generation profile is of the form

$$G_{op} = \alpha\, X\, L_{fl} e^{-\alpha x} \quad (10)$$

where X is the solar concentration as defined above and L_{fl} is the flux of above band gap photons.

We consider our recombination rate U as an addition process of three independent types: radiative, Shockley-Read-Hall (SRH), and Auger recombination rates. All three rates depend on how far the carrier densities are from the equilibrium value: $np - n_i^2$. The radiative recombination rate

$$U_{rad} = R_{ec}(np - n_i^2) \quad (11)$$

depends on the radiative recombination constant R_{ec} (6.41×10^{-14} cm^3/s). The SRH recombination rate

$$U_{SRH} = \frac{np - n_i^2}{\tau_n\left(p + n_i e^{\frac{E_i - E_T}{kT}}\right) + \tau_p\left(n + n_i e^{\frac{E_T - E_i}{kT}}\right)} \quad (12)$$

considers a single trap energy level, E_T, with electron and hole lifetimes, τ_n (0.323×10^{-6} seconds) and τ_p (52.6×10^{-6} seconds), respectively, to determine the rate [9]. The Auger recombination rate

$$U_{Aug} = (A_n n + A_p p)(np - n_i^2) \quad (13)$$

depends on A_n and A_p, the Auger constants for germanium. Since each type of recombination is independent of each other, we can define the total recombination rate as

$$U = U_{rad} + U_{SRH} + U_{Aug}. \quad (14)$$

C. Finite-element method and Boundary Conditions

To solve our PDE system, we use a finite-element method (FEM), Newton's Method, and nested iteration to numerically approximate solutions. The equations are written in weak form and boundary conditions (BCs) are applied at the beginning and end of the device depth, x=0 and x=L, to complete the system. This non-linear variational system is linearized via Newton's Method to iteratively approximate the solution on a hierarchy of grids with increasing resolution [7].

We use Neumann BCs for the electric potential, where the value of the derivative is imposed on the boundary. We weakly constrain the derivative of the potential – the electric field, ξ – to be zero, which allows the electric potential to evolve more naturally with the changing solar concentrations [8].

$$\xi(0) = \frac{\partial V}{\partial x}|_{x=0} = 0 \tag{15}$$

$$\xi(L) = \frac{\partial V}{\partial x}|_{x=L} = 0 \tag{16}$$

For our carrier concentrations, we set the flux of the carriers to be zero at the boundary to represent the conditions at V_{OC}. We do this by using Robin BCs, which constrain the derivative to a value of the function at the endpoints. Surface recombination effects, S_r, help define the Robin BCs [10].

$$\frac{\partial n}{\partial x}|_{x=0} = \frac{S_r}{D_n}(n(0) - n_0) \tag{17}$$

$$\frac{\partial n}{\partial x}|_{x=L} = -\frac{S_r}{D_n}(n(L) - n_0) \tag{18}$$

$$\frac{\partial p}{\partial x}|_{x=0} = \frac{S_r}{D_p}(p(0) - p_0) \tag{19}$$

$$\frac{\partial p}{\partial x}|_{x=L} = -\frac{S_r}{D_p}(p(L) - p_0) \tag{20}$$

Since the value of the electric field at the boundaries is zero, there is no drift component to the current. Therefore, the above equations state that any carrier that diffuses to the boundary must recombine there through a surface trap state.

III. Results

A. Evolution of V_{OC} with Solar Concentration (X)

We ran our original and GMR solvers at a series of increasing solar concentrations (X=1-10,000) and extracted V_{OC} from the quasi-Fermi levels computed from our carrier densities. Fig. 2 demonstrates that our GMR method is in good agreement with our original solver and at ultra-high levels of solar concentration, Auger recombination processes dominate and as a result limit V_{OC}. Our computed values for V_{OC} can be fit to (1) with a diode ideality factor that represents low-level injection (n=1) up to ~100 suns solar concentration. At higher solar concentrations, the results fit n=2/3, representing Auger recombination processes dominating. Our results are in very good agreement with previous work done on Ge solar cells at ultra-high solar concentration with the commonly employed device simulation software PC1D [5, 11], demonstrating the validity of our method of implementing the problem and that (1) seems to hold at higher concentrations.

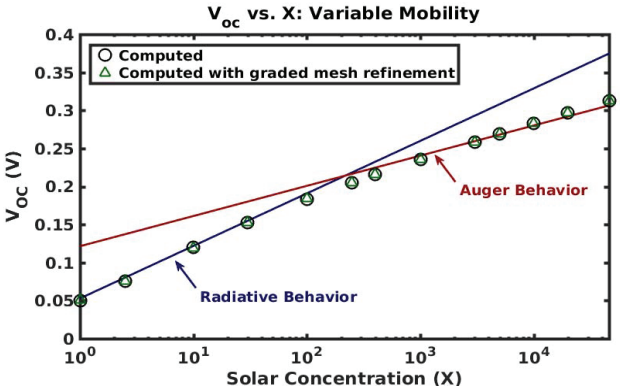

Fig. 2 V_{OC} as a function of solar concentration (X). Fit for computed data with and without graded mesh refinement based on different recombination mechanisms dominating. Both versions of our solver are in good agreement with previous ultra-high concentration work in the literature [5].

Fig. 3 shows our solutions under 1 sun solar concentration and 1000 suns solar concentration. As we increase the intensity of light on our device, we see an increase in optically generated carriers in the less doped p-type region of the device (x>0.3μm). At 1000 suns, it becomes difficult to distinguish between majority and minority carriers in the p-type region, as $\delta n \approx \delta p$. To investigate this phenomena further, we took a closer look at the quasi-Fermi levels of the carriers. We define an "average" quasi-Fermi level for the device to help us differentiate between the n-type and p-type regions once the distinction between majority and minority carriers is less clear.

$$\frac{E_{Fn}+E_{Fp}}{2} = \frac{2E_i + kT\ln\left(\frac{n_0+\delta n}{p_0+\delta p}\right)}{2}. \tag{21}$$

If $n_0 + \delta n < p_0 + \delta p$, the above expression shows the material is p-type,

$$\frac{E_{Fn}+E_{Fp}}{2} < E_i\,. \tag{22}$$

If $\delta n \approx \delta p \geq \max(n_0, p_0)$, the above expression shows the material is quasi-intrinsic,

$$\frac{E_{Fn}+E_{Fp}}{2} \approx E_i\,. \tag{23}$$

By plotting the average quasi-Fermi level with the intrinsic Fermi level (E_i), we clearly see the n-type and p-type regions of our device at 1 sun solar concentration, with the PN-junction marked by the crossover point of these two functions.

However, when we increase the solar concentration to 1000 suns, so that $\delta n \approx \delta p$ in the low-doped region, we lose our distinct barriers between the n-type and the p-type materials. In fact, the region where there are equal optically generated carriers (x>0.3μm) appears to be intrinsic. This could impact device performance in experimental work, as photovoltaic devices are designed with a specific built-in voltage to efficiently sweep carriers away from where they are generated to prevent recombination from occurring. Inefficient carrier extraction could be leading to the increased Auger recombination seen by Vossier et al. in their PC1D simulations [5]. Combined with the increase in thermally generated carriers arising from below band gap absorption, this could be exacerbating the degradation of V_{OC} that occurs due to thermal effects [6].

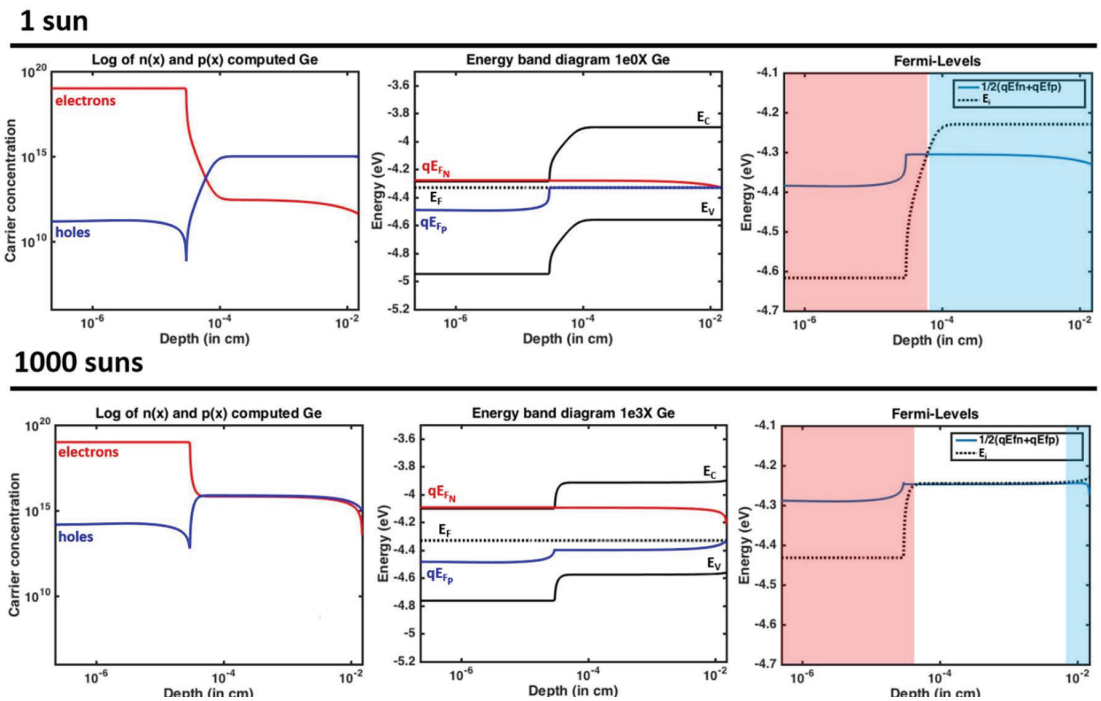

Fig. 3 Computed results for 1 sun solar concentration (top) and 1000 suns solar concentration (bottom). Left: carrier concentration profiles (units of cm^{-3}). At 1000 suns solar concentration the electrons and holes are of similar order of magnitude in the less doped p-type region. Middle: energy band diagrams showing the quasi-Fermi levels for each carrier. Right: further analysis of quasi-Fermi-levels to identify regions of n-type (red) and p-type (blue) behavior in the device.

IV. Conclusions

In this work, we presented our drift-diffusion and Poisson solver that uses a finite-element method and graded mesh refinement to study carrier dynamics under ultra-high solar irradiation. We analyzed the validity of previously used approximations on V_{OC} and the effects of increasing optically carrier densities on germanium solar cells. Although we find our simulations fit the previously employed assumption for V_{OC} (X) quite well, we point out a change in the carrier profiles that may be compounding with undesirable thermal effects and impacting experimental electrical properties. Future work will involve adding in thermal behavior to improve our model.

Acknowledgment

This work was supported but the Tufts Collaborates Seed Grant Program. M. Stevens acknowledges support from the NASA Space Technology Research Fellowship (NASA #NNX15AQ79H). M. Stevens and E. Carlson acknowledge support from the NSF STEM Leader Program (NSF EEC-1444926).

References

[1] M. A. Green, K. Emery, Y. Hishikawa, W. Warta, and E. D. Dunlop, "Solar cell efficiency tables (version 48)," *Prog. Photovoltaics Res. Appl.*, vol. 24, no. 7, pp. 905–913, Jul. 2016.

[2] M. Stevens, C. Downs, D. Emerson, J. Adler, S. Maclachlan, and T. Vandervelde, "Studying Anomalous Open-Circuit Voltage Drop-Out in Concentrated Photovoltaics Using Computational Numerical Analysis," in *Photovoltaic Specialists Conference (PVSC)*, New Orleans, LA, 2015.

[3] R. R. King, D. C. Law, K. M. Edmondson, C. M. Fetzer, G. S. Kinsey, H. Yoon, R. A. Sherif, and N. H. Karam, "40% efficient metamorphic GaInPGaInAsGe multijunction solar cells," *Appl. Phys. Lett.*, vol. 90, no. 18, pp. 90–93, 2007.

[4] D. J. Friedman and J. M. Olson, "Analysis of Ge junctions for GaInP/GaAs/Ge three-junction solar cells," *Prog. Photovoltaics Res. Appl.*, vol. 9, no. 3, pp. 179–189, 2001.

[5] A. Vossier, B. Hirsch, and J. M. Gordon, "Is Auger recombination the ultimate performance limiter in concentrator solar cells?," *Appl. Phys. Lett.*, vol. 97, no. 19, 2010.

[6] A. Braun, B. Hirsch, A. Vossier, E. A. Katz, and J. M. Gordon, "Temperature dynamics of multijunction concentrator solar cells up to ultra-high irradiance," *Prog. Photovoltaics Res. Appl.*, vol. 21, no. 2, pp. 202–208, 2013.

[7] D. Vasileska and S. M. Goodnick, "Computational Electronics," *Synth. Lect. Comput. Electromagn.*, vol. 38, pp. 181–236, 2002.

[8] M. Stevens, C. Downs, D. Emerson, J. Adler, S. Maclachlan, and T. E. Vandervelde, "Predicting Voc at Ultra-High Solar Concentration Using Computational Numerical Analysis," in *31st European Photovoltaic Solar Energy Conference and Exhibition*, Hamburg, Germany, 2015, pp. 1474–1477.

[9] J. Nelson, *The Physics of Solar Cells*, 1st ed. Imperial College Press, 2003.

[10] S. M. Sze, *Physics of Semiconductor Devices*, 3rd ed. Wiley-Interscience, 2007.

[11] D. A. Clugston and P. A. Basore, "PC1D version 5: 32-bit solar cell modeling on personal computers," *Conf. Rec. Twenty Sixth IEEE Photovolt. Spec. Conf. - 1997*, pp. 207–210, 1997.